

Supporting information

Visible-light responsive hydrogen production from formate with the photoredox system using enzyme and colloidal platinum nanoparticles

Shintaro Yoshikawa^a and Yutaka Amao^{a,b*}

^a Graduate School of Science, Osaka Metropolitan University, 3-3-138 Sugimoto, Sumiyoshi-ku, Osaka 558-8585, Japan

^b Research Centre of Artificial Photosynthesis (ReCAP), Osaka Metropolitan University, 3-3-138 Sugimoto, Sumiyoshi-ku, Osaka 558-8585, Japan,

Email: amao@omu.ac.jp

1. Materials

Zinc meso-tetra(4-sulfonatophenyl)porphyrin tetrasodium salt (ZnTPPS⁴⁻) was purchased from Frontier Scientific, Inc. Colloidal platinum nanoparticles dispersed in polyvinylpyrrolidone (Pt-PVP) was purchased from Tanaka Holdings Co. Ltd. Pt concentration in Pt-PVP was estimated to be 4.0 wt.%. The particle size of Pt-PVP was estimated to be *c.a.* 2.0 nm using transmission electron microscope (TEM) image shown in the analysis table published by Tanaka Holdings Co., Ltd. NAD⁺ and NADH were purchased from Oriental Yeast Co., Ltd. Formate dehydrogenase from *Candida boidini* (CbFDH) was supplied by Merck Ltd. Methylviologen dichloride (MV²⁺) was purchased from Tokyo Chemical Industry Co., Ltd. The other chemicals were of analytical grade or the highest grade available purchased from Wako Pure Chemical Co. Ltd.

2. Experimental procedure

Add 5.0 mL of phosphate buffer containing sodium format, CbFDH, NAD⁺, ZnTPPS⁴⁻, MV²⁺ and Pt-PVP to a 17.2~19.3 mL total volume eggplant-type flask with a side tube and high vacuum stopcock as shown in Figure S1(a). A sample solution was deaerated by freeze-pump-thaw cycles (6 times) and flushed with Ar gas for 10 min. Then, the sample solution was irradiated with a 250 W halogen lamp as a visible-light energy source. The outline of the experimental setup is shown in Figure S1(b).

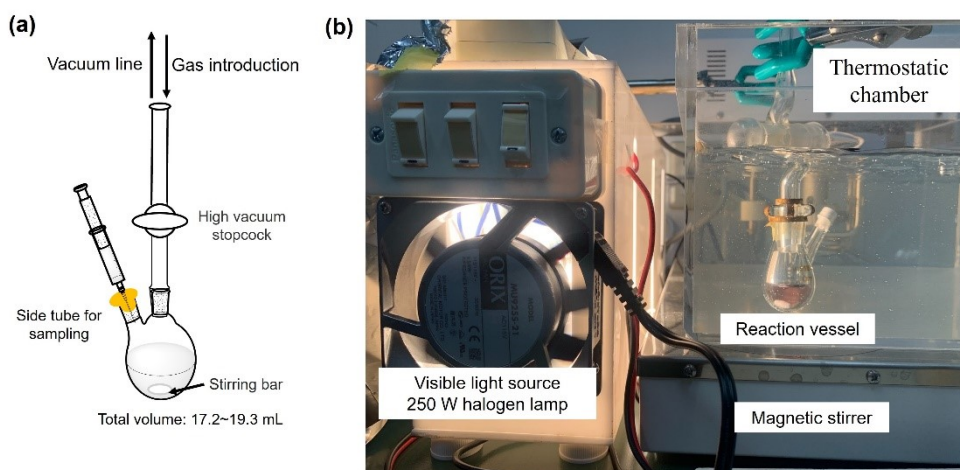


Figure S1. Outline of reaction vessel (a) and the experimental setup (b)

3. Determination for formate concentration using ion chromatography

The amount of formate was detected using ion chromatography system (Metrohm, Eco IC; electrical conductivity detector) with an ion exclusion column (Metrosep Organic Acids 250/7.8 Metrohm; column size: 7.8 x 250 mm; composed of 9 μm polystyrene-divinylbenzene copolymer with sulfonic acid groups). The 1.0 mM perchloric acid and 50 mM lithium chloride in aqueous solution were used as an eluent and a regenerant, respectively. Flow rate of eluent solution was adjusted to be 0.5 mL min^{-1} . The retention time for formate was detected at 13.5 – 15.0 min. The electrical conductivity changes in the various formate concentrations (0 – 100 mM) were shown in Figure S2. As shown in Figure S2, the retention time of the peak position shifts with increasing formate concentration. Inset of Figure S1 shows the relationship between the formate concentration and the detection peak area using ion chromatograph.

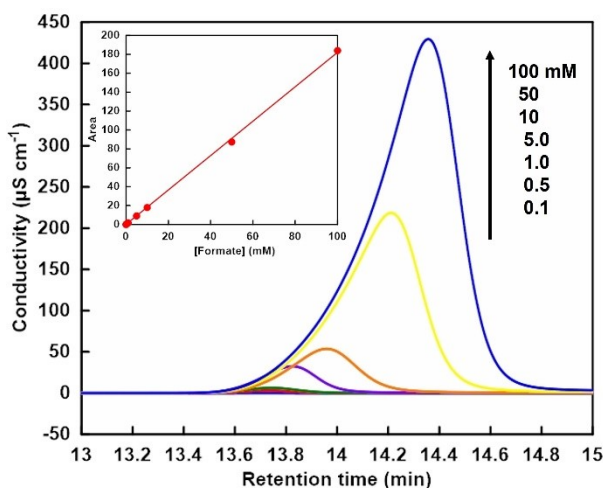


Figure S2. Chromatogram of formate (0 – 100 mM) in 500 mM-HEPES buffer (pH 7.0). Inset: Relationship between the formate concentration and the detection peak area.

As shown in the inset of Figure S2, the formate concentration and the detected peak area showed a good linear relationship (correlation coefficient: $r^2=0.998$) as following equation (S1).

$$\text{Peak area} = 1.8 \times [\text{formate}](\text{mM}) \quad (\text{S1})$$

4. Determination of hydrogen and carbon dioxide using gas chromatography

The amount of hydrogen and carbon dioxide production was determined by gas chromatograph (GC-2014, SHIMADZU Corporation) with a thermal conductivity detector (TCD). Activation charcoal column (column length: 3 mm I.D. × 2 m) was equipped for detecting sample gas. The temperature of injection, column and detector were adjusted to be 100.0, 70.0 and 100.0 °C respectively. Ar gas was used by carrier gas and the flow rate was 30.0 mL min⁻¹. The retention time for hydrogen was detected at 0.9 – 1.5 min. The signal intensity changes in the various amount of hydrogen (0 – 2.2 μmol) were shown in Figure S3.

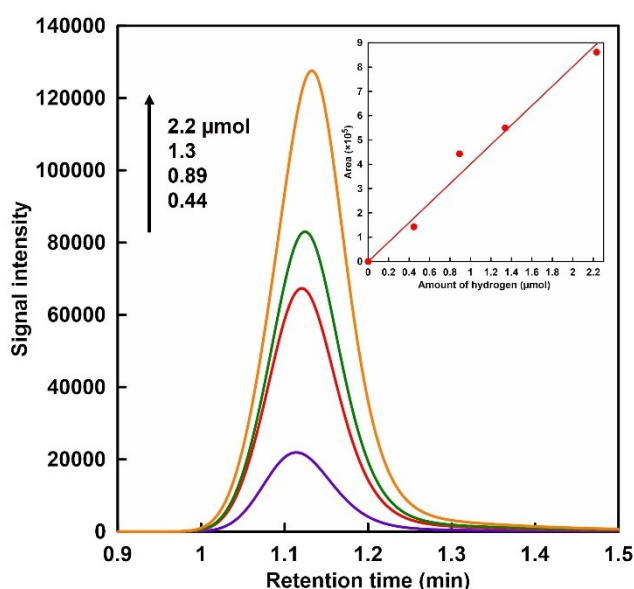


Figure S3. Chart of chromatogram of hydrogen (0 – 2.2 μmol). Inset: Relationship between the amount of hydrogen and the detection peak area.

As shown in the inset of Figure S3, the amount of hydrogen and the detected peak area showed a good linear relationship (correlation coefficient: $r^2=0.992$) as following equation (S2).

$$\text{Peak area} = 4.9 \times 10^5 \times \text{hydrogen } (\mu\text{mol}) \quad (\text{S2})$$

The retention time for carbon dioxide was detected at 15.5-20.0 min. The signal intensity changes in the various amount of carbon dioxide (0 – 2.2 μmol) were shown in Figure S4.

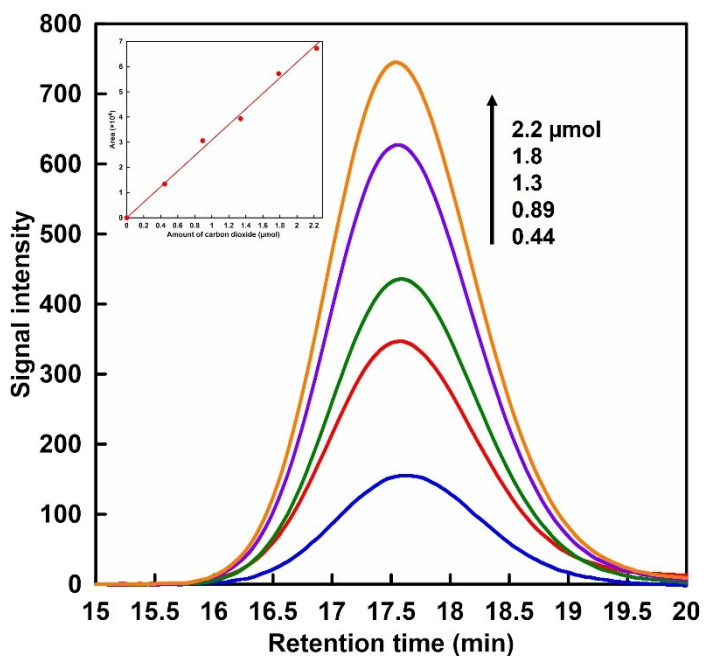


Figure S4. Chart of chromatogram of carbon dioxide (0 – 2.2 μmol). Inset: Relationship between the amount of carbon dioxide and the detection peak area.

As shown in the inset of Figure S4, the amount of carbon dioxide and the detected peak area showed a good linear relationship (correlation coefficient: $r^2=0.998$) as following equation (S3).

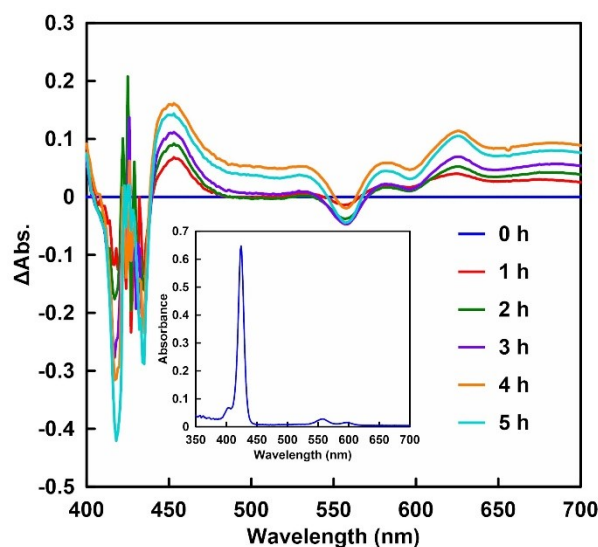
$$\text{Peak area} = 3.1 \times 10^4 \times \text{carbon dioxide } (\mu\text{mol}) \quad (\text{S3})$$

5. Hydrogen and carbon dioxide production with the system of sodium formate, CbFDH, NAD⁺, ZnTPPS⁴⁻, MV²⁺ and Pt-PVP during irradiation

The sample solution consisted of sodium formate (50 μmol) CbFDH (0.95 U; *c.a.* 24 nmol), NAD⁺ (25 μmol), ZnTPPS⁴⁻ (50 nmol), MV²⁺ (0.25 μmol) and Pt-PVP (0.25 μmol) in 5 mL of 200 mM phosphate buffer. Hydrogen and carbon dioxide produced were analysed using gas chromatograph and formate consumption was analysed using ion chromatograph. The pH of the reaction samples was adjusted using phosphate buffering capacity.

6. UV-vis absorption spectral changes in the sample solution of sodium formate, CbFDH, NAD⁺, ZnTPPS⁴⁻, MV²⁺ and Pt-PVP during irradiation

Figure S5 shows the time dependence of difference spectra in the sample solution of sodium formate, CbFDH, NAD⁺, ZnTPPS⁴⁻, MV²⁺ and Pt-PVP in phosphate buffer (pH 7.0) from before to after light irradiation (inset: UV-vis absorption spectrum of



ZnTPPS⁴⁻).

Figure S5. Time dependence of difference spectra in the sample solution of sodium formate (50 μmol) CbFDH (0.95 U; *c.a.* 24 nmol), NAD⁺ (25 μmol), ZnTPPS⁴⁻ (50 nmol), MV²⁺ (0.25 μmol) and Pt-PVP (0.25 μmol) in 5 mL of 200 mM phosphate buffer (pH 7.0) from before to after light irradiation. Inset: UV-vis absorption spectrum of ZnTPPS⁴⁻ in buffer solution.

The reduced concentration of ZnTPPS⁴⁻ was calculated from absorbance change at 555 nm based on the molar absorption coefficient ($\epsilon=16,000 \text{ M}^{-1} \text{ cm}^{-1}$).

Evaluation of the tolerance of CbFDH during long periods irradiation

After 25 h of irradiation, sodium formate (50 μmol) was added to the sample solution and irradiation was continued again. The concentration of formate consumption was analysed using ion chromatograph. Figure S6 shows the time dependence of formate consumption during irradiation.

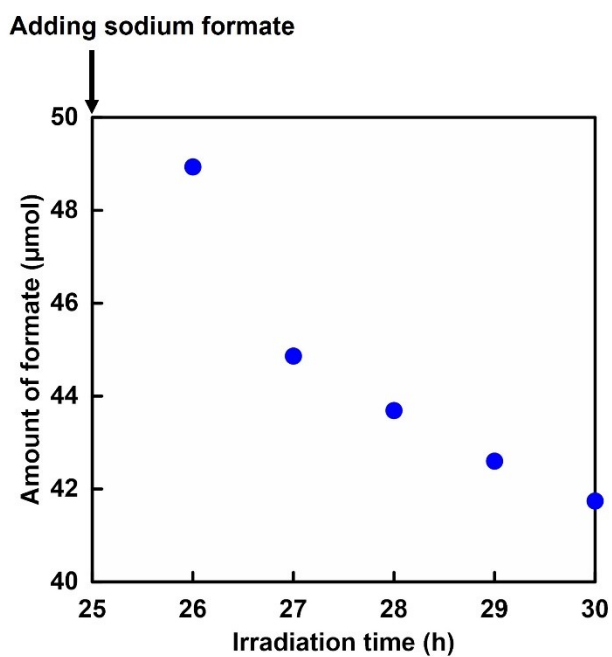


Figure S6. The time dependence of formate consumption during irradiation.

7. Hydrogen and carbon dioxide production with the system of sodium formate, CbFDH, NAD⁺, ZnTPPS⁴⁻, MV²⁺ and Pt-PVP during irradiation more than 500 nm

The sample solution consisted of sodium formate (50 μmol) CbFDH (0.95 U; *c.a.* 24 nmol), NAD⁺ (25 μmol), ZnTPPS⁴⁻ (50 nmol), MV²⁺ (0.25 μmol) and Pt-PVP (0.25 μmol) in 5 mL of 200 mM phosphate buffer (pH 7.0). The sample solution was irradiated through optical filter Y52(HOYA). Hydrogen and carbon dioxide produced were analysed using gas chromatograph. Figure S7(a) shows the time dependence of hydrogen and carbon dioxide production during irradiation through optical filter Y52(HOYA). Figure S7(b) shows the transmittance characteristics of optical filter Y52 and UV-vis absorption spectrum of ZnTPPS⁴⁻.

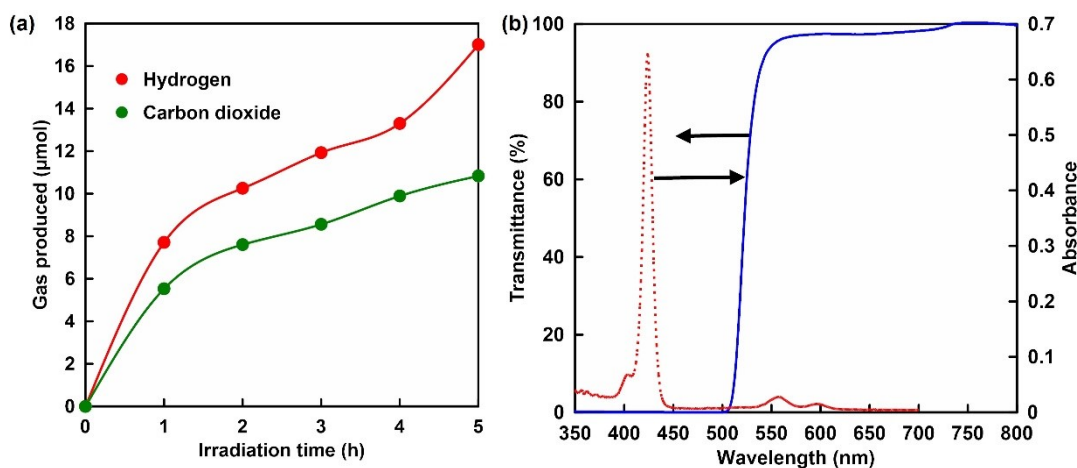


Figure S7. The time dependence of hydrogen and carbon dioxide production during irradiation through optical filter Y52(HOYA) (a) and the transmittance characteristics of optical filter Y52 and UV-vis absorption spectrum of ZnTPPS⁴⁻ (b).

8. CbFDH catalysed formate oxidation in the presence of NAD⁺ under various pH conditions

The sample solution of sodium formate (10 mM), NAD⁺ (0 – 5.0 mM) and CbFDH (0.95 U; *c.a.* 4.8 μM) in 5.0 mL of phosphate buffer solution (pH 6.0 - 8.0) was incubated at 30.5 °C. The reaction is carried out using the shaking incubator with a thermostatic chamber (EYELA NTS-4000, TOKYO RIKAKIKAI Co. Ltd.). The reaction temperature is adjusted at 30.5 °C. The shaking speed is adjusted to be 80 rpm. The apparent formate oxidation was calculated by the absorbance change at 340 nm with a molar absorption coefficient of NADH ($\epsilon_{340} = 6300 \text{ M}^{-1} \text{ cm}^{-1}$) using UV-visible absorption spectroscopy (HITACHI U-2910) as equivalent to the concentration of NADH produced during reaction. The reaction rate (v) was calculated from the gradient of the NADH production up to 30 s incubation. Figure S8 shows the relationship between the initial concentration of NAD⁺ and the reaction rate for NADH production due to formate oxidation with CbFDH under various pH conditions.

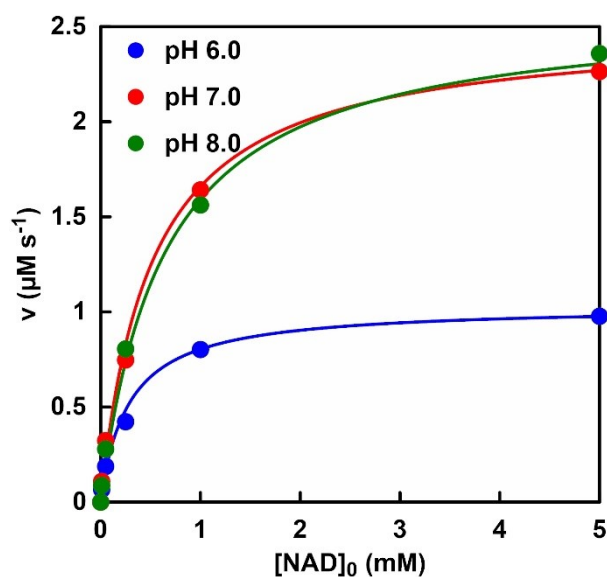


Figure S8. The relationship between the initial concentration of NAD⁺ and the reaction rate for NADH production due to formate oxidation with CbFDH under various pH conditions.